JBAAR

Journal of Bioscience and Applied Research
https://jbaar.journals.ekb.eg

SPBH

Characterization of *Paramyrothecium roridum* isolated from soil

***Janan K. Al-Tarjuman[1], Faten N. Mula Abed[2] and Fahad K. Y. AL-Dulaimi[1]**

[1] Northern Technical University, College of Agricultural Technology, Plant Production techniques Mosul, Iraq.

[2] College of Science, Mosul University, Iraq.

*Corresponding author: Janan K. Al-Tarjuman, Email: janankhorshed@ntu.edu.iq

DOI:10.21608/jbaar.2024.309341.1062

Abstract

The fungus *Paramyrothecium roridum* (Tode) L. Lombard and Cross, previously known as *Myrothecium roridum* Tode ex Fries, belong to the family Stachybotriaceae and are species of *Myrothecium* distributed worldwide in soil and decaying plant tissues as saprophytic fungi or pathogens on diverse hosts. The morphology of the asexual morph, particularly the characteristics of conidia and conidiophores, was previously used to classify species in this genus because few features distinguish species within a genus, and morphology-based identification alone is inaccurate; consequently, DNA sequence data are useful for identifying species. Fungal isolation was identified according to morphological characteristics. In Potato Dextrose Agar (PDA) culture, the olive-green conidia were 6-6.5 µm long × 2.3 µm wide, and cylindrical with rounded ends. Conidia formed dark green to black masses on sessile sporodochia in concentric zones, as well as identified based on a molecular approach using a polymerase chain reaction assay (PCR) of internal transcribed spacer *(ITS1 5.8S ITS2)* of the rDNA to confirm the *Paramyrothecium roridum* using primers (ITS1 and ITS4). The produced band size was 600 bp. The nucleotide sequences of the amplification products were analyzed, and the results confirmed *the diagnosis of Paramyrothecium roridum.* As a result, the isolate *Paramyrothecium roridum* was recorded as a JFF22 isolate in the National Centre for Biotechnology Information (NCBI) for the first time in Iraq.

Keywords: *Paramyrothecium roridum*, media, Polymerase chain reaction, Morphological identification, Scanning electron micrograph.

Introduction

Tode (1790) introduced the genus *Myrothecium* and listed five species: *M. roridum, and M. inundatum, as* well as three more species that Fries (1829) subsequently claimed belonged to different genera. (l) *Myrothecium* species are members of the fungal family Stachybotriaceae, and more than 30 species of the fungus have been identified till 2011 (2). The genus *Myrothecium* has a broad range of hosts, including more than 300 plant species of field crops, ornamental plants, and vegetables. This fungus grows in soil and mainly affects the foliar sections of its host, causing fruit to rot in some hosts as well as leaf spots and stem lesions (3). *P. roridum* can also be spread by the seeds of several plant species (4). Leaf spots on crops like lamb's lettuce, pepper, watermelon, and soybean, as well as many ornamentals, have been reported in many different countries due to *P. roridum* infection (5-13). Species *of Myrothecium* oftentimes subsist in the environment as endophytes and/or saprophytes on decayed and dead plant tissue (14), but some species as the well-known plant pathogen *Myrothecium roridum* Tode and the mild pathogen *M. verrucaria* Ditmar (15). The first Myrothecium-related disease was discovered in America on a tomato (16).

Received: August 3, 2024. Accepted: November 5, 2024. Published: November 14, 2024

Myrothecium species have been recorded as coffee pathogens (17), soybean seeds, rice, chili seed, and mulberry (16, 18). Various economically significant crops such as root rot in red clover (19), leaf blight in cotton (20), Peanut (21); leaf spot in pepper, tomato, cotton, cucurbits, lamb lettuce, cotton (6, 7,22), and potato (15), are also grown. Proper attention to watering and soil hygiene is essential for minimizing crop damage because the development of Myrothecium-caused plant diseases is typically related to wet soil conditions (23). Myrothecium is a genus of Deuteromycetes that includes several species that inhabit soils, and some of these species are capable of producing antibiotics like Myrocin C and other bioactive compounds (24). The positive aspects of Myrothecium species involve compounds that can inhibit liver cancer and promyelocytic leukemia cell activity as well as tumor activity (25-27) and produce bioactive secondary metabolites; *M. roridum* has reported more than 20 compounds, and *M. verrucaria* has reported more than 30 compounds (28,16). In addition, many macrocyclic trichothecene mycotoxins, including verrucarin and roridin, are produced by Myrothecium species (29-31). If the therapeutic potential of Myrothecium species is further investigated, this treatment may benefit human health.

Materials and Methods:

Fungal isolation

Myrothecium roridum was isolated from soil samples collected from northern Iraq, Nineveh governorate, Mosul city, during spring 2019, using Rose Bengal chloramphenicol agar (RBC) which consists of: (peptone; Glucose; Dipotassium phosphate; Magnesium sulfate; Rose Bengal; Agar and chloramphenicol) at concentration (5, 10, 1, 0.5, 0.05, 15,100) gm/l sequentially (32) as growth medium. Soil sprinkle plates and soil dilution were employed as methods for isolating microorganisms. The sprinkle plates involved directly spreading soil onto the medium surface and incubating it at 25°C for a week. To create soil dilutions, 1 g of each soil sample was suspended in 50 ml of sterile distilled water. After stirring these suspensions for 20 min, 0.1 ml of each was distributed onto the medium on the plates using seven-fold falling dilutions. The plates were then incubated for 7 days at 25 °C. Sub-culturing was used to move the fungi that were developing on the agar plates from hyphal tips, colonies, or spores to a new potato Dextrose Agar (PDA) plate to obtain a pure culture of the associated fungus (33).

Morphological identification

Morphological features such as colony color and texture, conidial color and shape, conidiophores cells, and sporodochia color were examined accurately to identify the fungal isolate (34,35).

Slide culture

The best method for definitive identification of fungal reproductive structure and mycelia is the slide culture technique described by Riddle, 1950(36), which requires a glass rode in the shape of the letter (V) placed inside a sterile glass petri plate containing a sterile filter paper, an agar block media (PDA) cut with a sterile scalpel installed over a glass slide and transferred on the glass rode, by sterile wire needle the fungus inoculated to the four sides of the agar block from the culture plate, the inoculated media block was covered with coverslip and pressured slightly to ensure adherence. Approximately 2 mL of sterile water was dropped on the bottom of a Petri plate, and the plate cover was replaced and incubated at 25 ^{0}C.

Molecular identification of *Paramyrothecium roridum*

Genomic DNA extraction and polymerase chain reaction (PCR)

For genomic DNA of *Paramyrothecium roridum*, *the* fungal isolate was cultured on Potato Dextrose Agar medium for 7 days at 25^{0}C. Mycelia were harvested, and extraction was performed using (ZR Fungal/Bacterial/ Yeast DNA MiniPrep™, Catalogue No. D6005, USA) according to the manufacturer's instructions. The ITS rDNA region

was amplified using the universal primer sets ITS-1 (5'-TCC GTA GGT GAA CCT GCG G-3') and ITS-4 (5'-TCC TCC GCT TAT TGA TAT GC-3') (37). PCR amplification was performed in a total volume of 25µl with 1.5µl DNA, 5 µl Taq PCR PreMix (Intron, Korea), 1µl of each primer (10 pmol), and distilled water to a total volume of 25µl. The thermal cycling conditions included denaturation at 94 °C for 3 min, followed by 35 cycles of 94 °C for 45s, 52°C for 45s, and 72 °C for 45s, with a final incubation at 72 °C for 7 min using a thermal Cycler (Gene Amp, PCR system 9700; Applied Biosystem). The PCR products were separated by 1.5% agarose gel electrophoresis and visualized under ultraviolet light (302nm) following red staining (Intron Korea).

Sequencing and Sequence Alignment

Macrogen Korea performed gene sequencing, followed by a homology search using the BLAST program available at NCBI online and the BioEdit program. PCR products were purified and sequenced using the BigDye Terminator v3.1 Cycle Sequencing kit on an ABI 3130 Genetic Analyser. The sequence was then analyzed in nucleotide databases using NCBI's BLAST Bio ID program to identify samples and submitted to GenBank (ID). Related sequences were obtained from NCBI's nucleotide database and included in multiple alignments using the Bio ID program (38,39).

Phylogenetic tree

The evolutionary history was inferred using the Neighbour-Joining method. The evolutionary distances were computed using the Jukes-Cantor model to determine the phylogenetic distance designed in the Geneous program.

Submission of the NCBI report

The 600 bp of partial 18S-ITS1-5.8S-ITS2 -28S rDNA sequence of the isolate *Paramyrothecium roridum* was submitted to NCBI registration, which passed the validations steps and was then used to create reference sequence entries.

Evaluation of the impact of culture media on the growth of *Paramyrothecium roridum* mycelium:

Four different cultural media were used to evaluate the fungal *Myrothecium roridum's* mycelial expansion. These cultural media included PDA that consists of Pieces of potatoes, dextrose, and agar at (200, 15, 20) g. Sabouraud agar medium(SA) includes glucose, peptone, and agar at (40,10, 15) g. Czapec-Dox agar medium (ZA) contains sodium nitrate, potassium nitrate, potassium chloride, magnesium sulfate, ferrous sulfate, sucrose, and agar (2, 1, 0.5, 0.5, 0.01, 30, 20) g. Malt extract agar (MEA) medium is made up of malt extract and 20 g of agar. The cultural medium was individually expressed in 1 L of distilled water and sterilized using an autoclave at 120°C under 15 psi pressure for 20 min. (Pitt and Hocking,2009) (38).

Evaluation of the effect of temperature on the growth of *Paramyrothecium roridum* mycelium:

To determine the effect of temperature on the mycelial growth of *Paramyrothecium roridum*, *Potato* Dextrose Agar was used as the culture medium. A disc of 5mm diameter from the edge of the pure culture was inoculated on PDA at four temperatures: 10, 20, 25, and 30 C. Colony growth was determined on day 7. Radial surface growth was recorded using two perpendicular diameters, and three replicates were performed for each temperature.

Results and Discussion

Paramyrothecium roridum isolation

Three soil samplings gathered from the Nineveh governorate, Mosul city, were analyzed for fungal inhabiting soils using soil sprinkle plates and the soil dilution method with the use of Rose Bengal chloramphenicol agar as media; only one isolate of *Paramyrothecium roridum* was obtained using soil sprinkle plates (Fig.1) and (Fig 2). To achieve a pure culture of the related fungus, we performed a subculture in which we transferred the fungi growing on the agar plates from hyphal tips, colonies, or spores to a fresh plate containing potato Dextrose Agar (PDA).

Fig. 1: Soil sprinkle plates for isolating fungal-inhabited soils

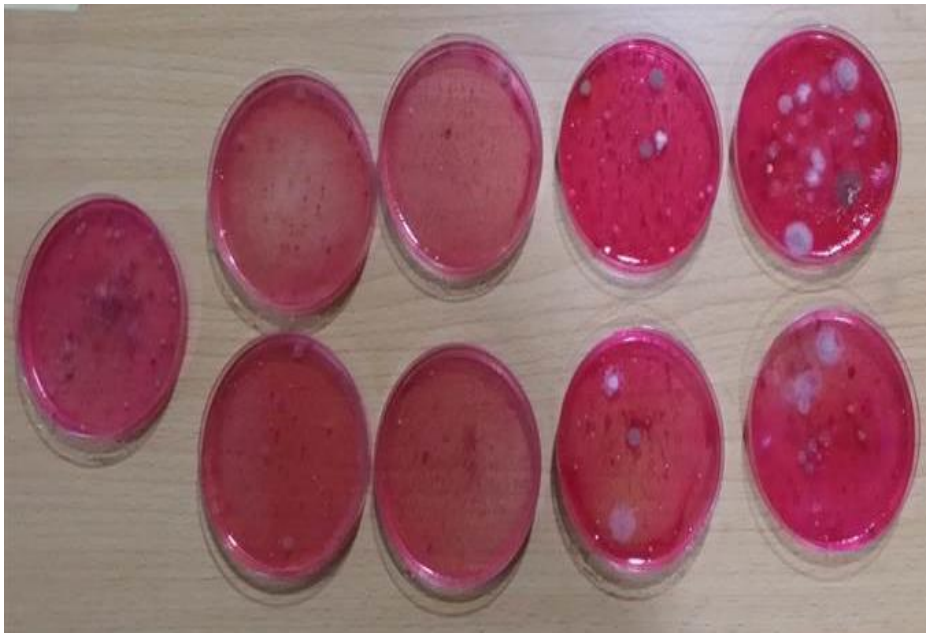

Fig. 2: Soil dilution method for isolating fungal-inhabited soils

Identification of *Paramyrothecium roridum*

Morphological identification

For morphological identification, the fungal isolate of *Paramyrothecium roridum* was grown on PDA and WWA for 7 days at 25^0C the colony patterns were photographed, and the colony was characterized on PDA with white mycelia slowly grew and looked wrinkled and reverse light yellow, after culturing over 10 days dark olivaceous – black sessile sporodochia radically spread above the mycelia, the microscopic examination of fungal isolate on PDA and WWA revealed that conidiophores were erect, arising from stroma, hyaline, and branched, each branch bear (Fig 3-10) phialide with a cylindrical shape where conidia were produced while the conidia were cylindrical shape with rounded ends, the conidial mass was green despite staining with lactophenol cotton blue, and the size of conidia was measured with the electron microscope (SEM) (conidia were generally 6.5 x 2.5(Fig 11-13).

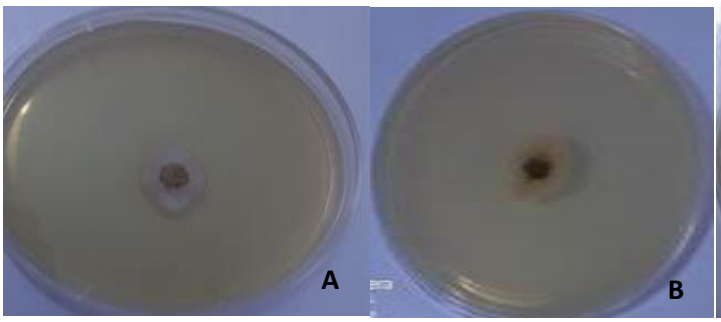

Fig (3): (A) Five-day colony morphology on potato dextrose agar. (B) The reverse of the plate appeared light yellow.

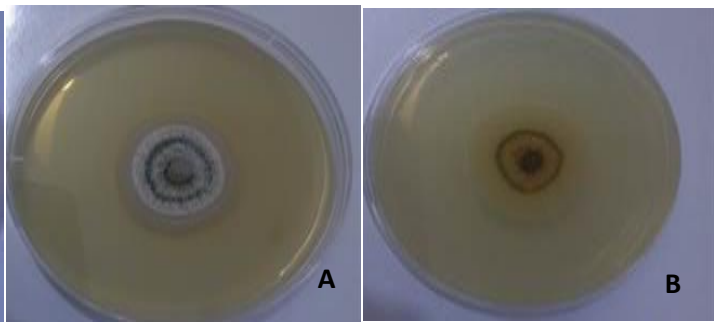

Fig (4): (A) 15-day colony morphology on potato dextrose agar. (B) The reverse of the plate appeared light yellow.

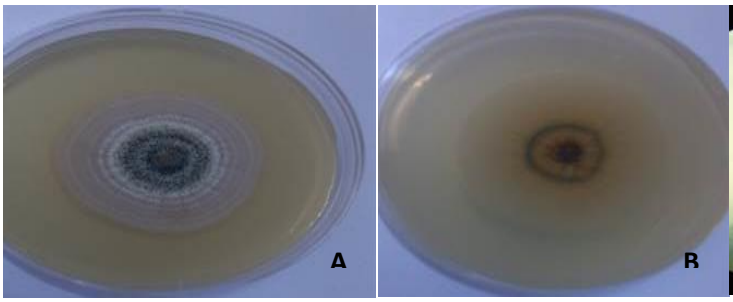

Fig (5): (A) 30-day colony morphology on potato dextrose agar. (B) The reverse of the plate appeared light yellow.

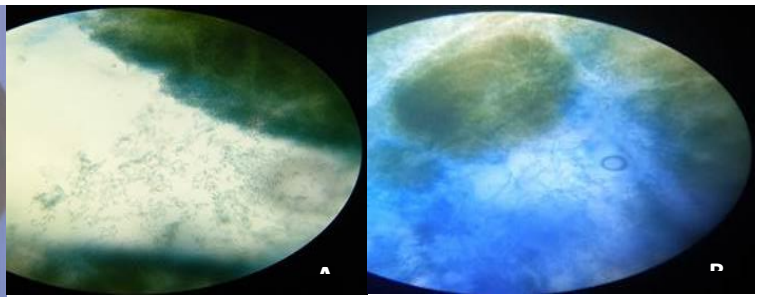

Fig (6): A and B, conidial masses

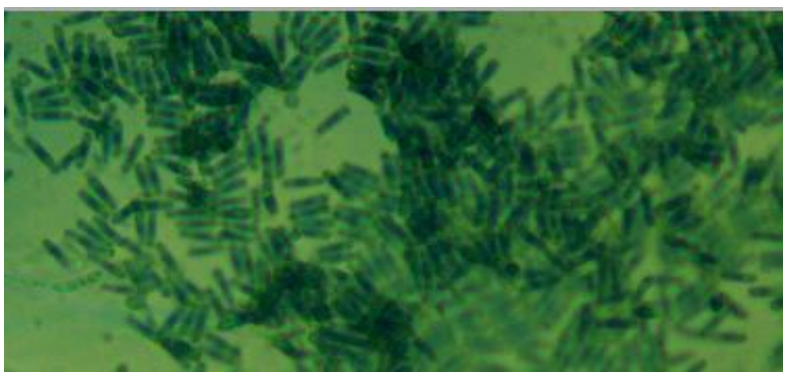

Fig (7): Radical conidia

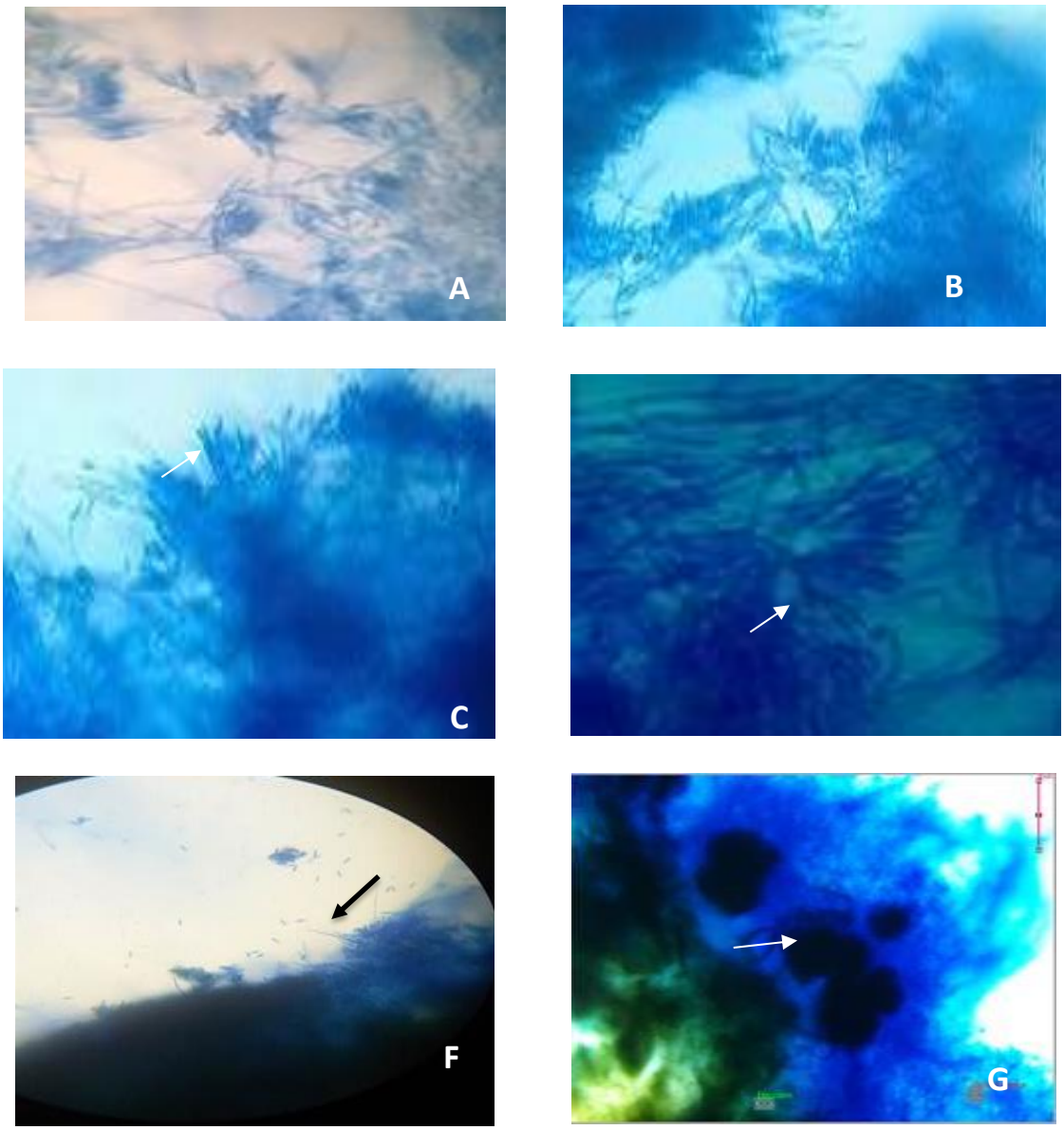

Fig (8): A - D, Conidiogenous cell, F: Setae, G: Sporodochia

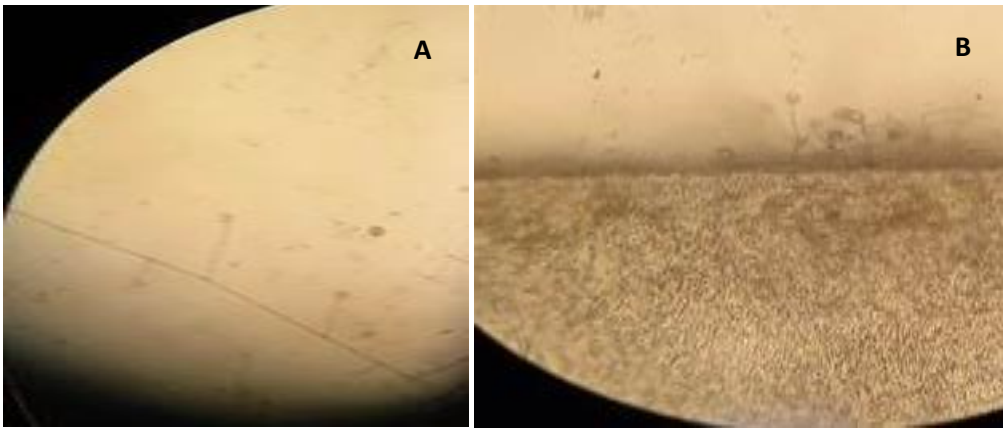

Fig (9) Slide culture technique: A and B: Conidiophores on PDA, C-F: Colony morphology on PDA with

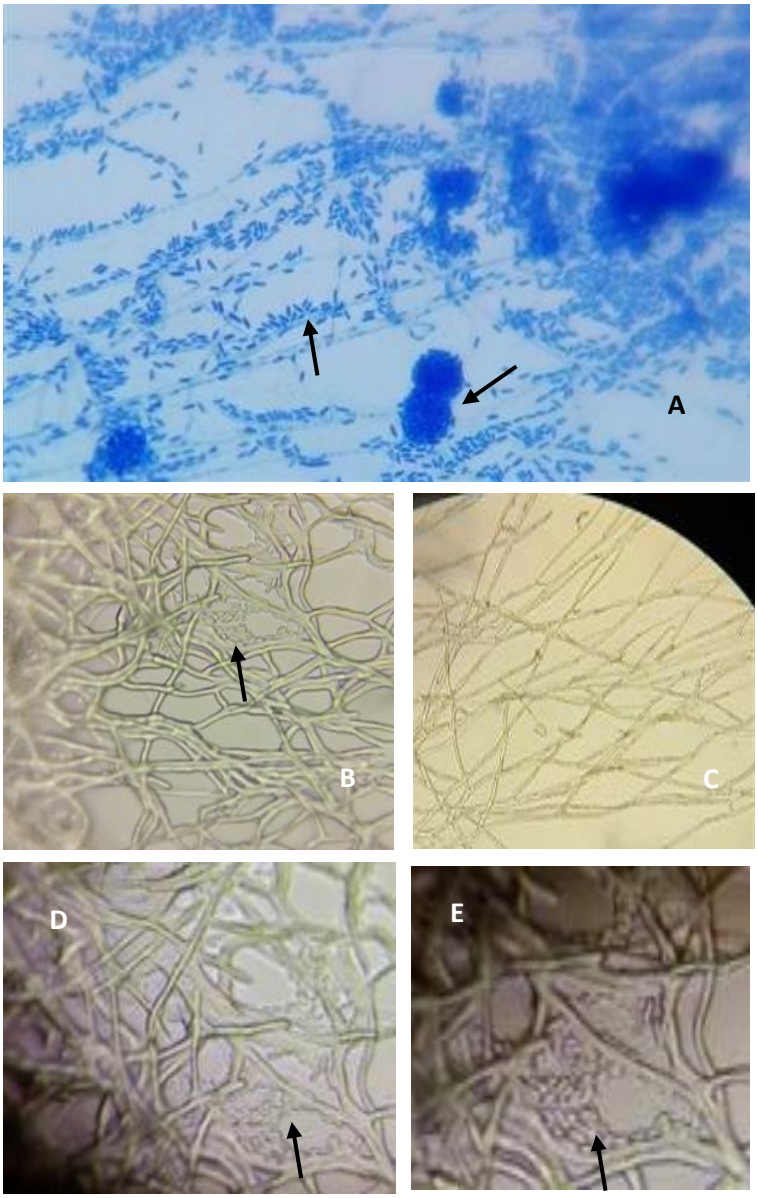

Fig (10): WWA: A: Conidia and spore clusters, B-E: microscopy images of mycelia and spores

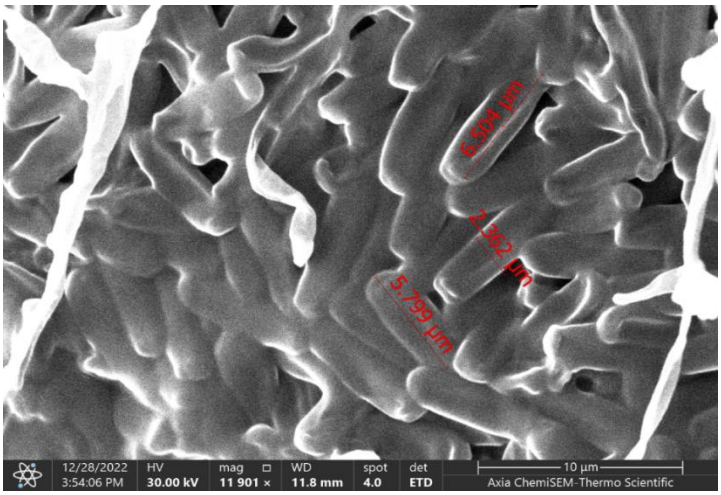

Fig (11): Scanning electron micrograph of Conidial mass of *Paramyrothecium roredium*

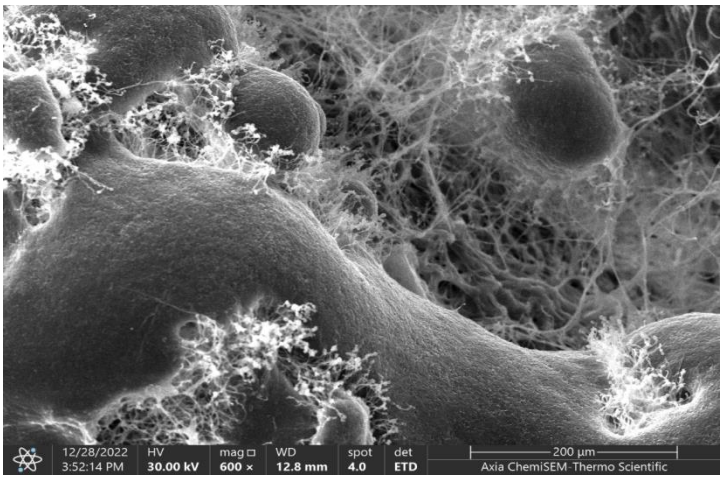

Fig (12): Scanning electron microscope (SEM) images show general aspect of sporodochia

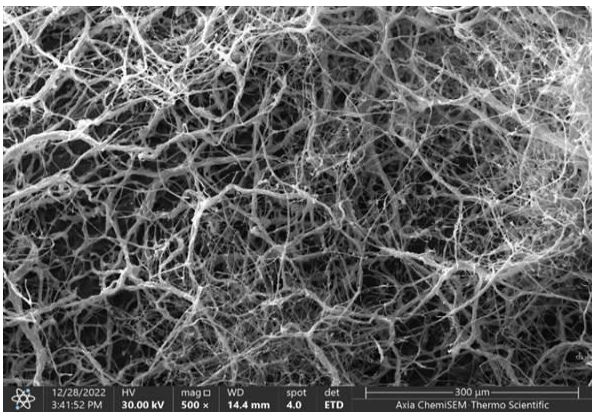

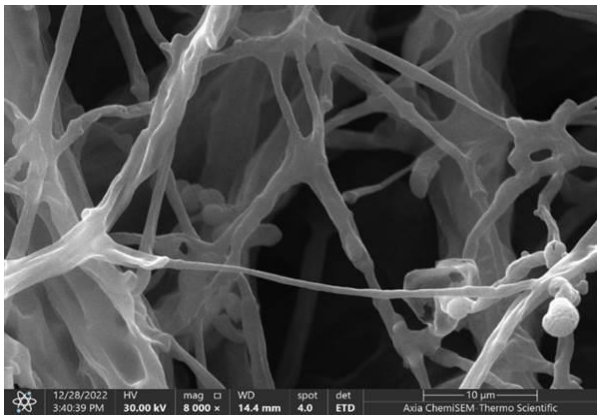

Fig (13): A and B Scanning electron microscopy of the fungus *Paramyrothecium soredium* (general view) showing dense network mycelium growing on PDA

To confirm the morphological identification of *Paramyrothecium roridum* isolates, PCR was employed for the identification of the ITS gene. After electrophoresis on agarose 2 %, the amplification results indicated that the size of the resulting bundle was 600 base pairs Fig (14 and 15).

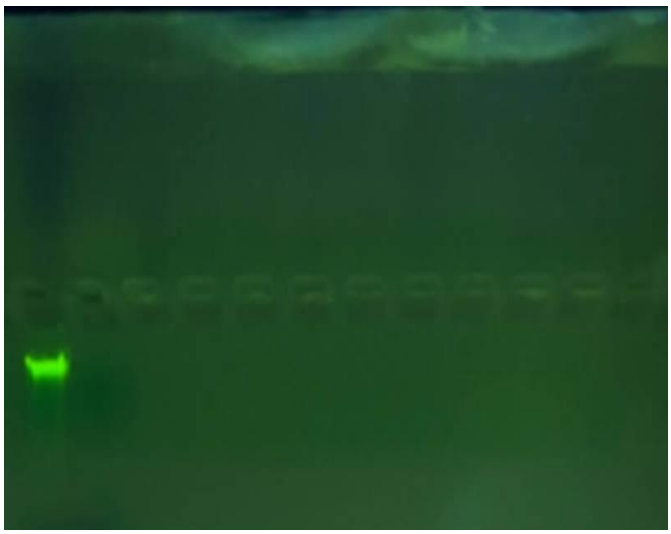

Figure (14): Genomic DNA extracted from the Fungal sample was subjected to gel electrophoresis on a 1% agarose gel, running at 5 volts per centimetre for 40 min.

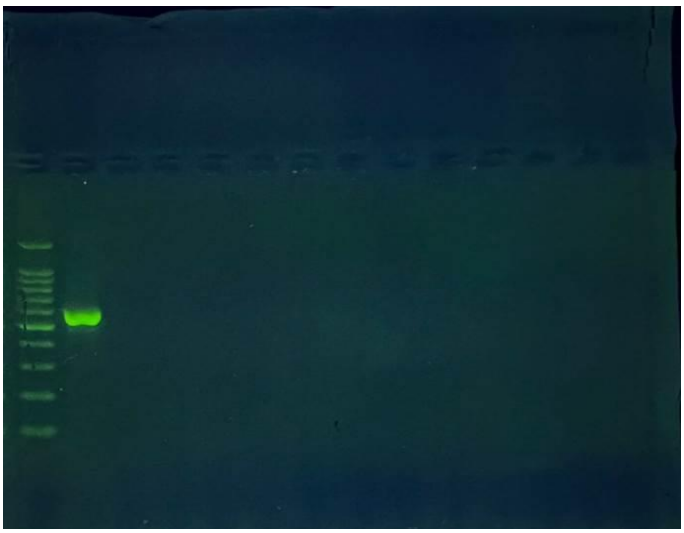

Figure (15): The PCR product exhibited a band size of 600 base pairs. The samples were subjected to electrophoresis on a 2% agarose gel at 5 volts per centimeter squared using 1x TBE buffer for a duration of 1 h. The DNA ladder used as a reference contained fragments of 100 base pairs.

Moumni et al. (2020) mentioned that the size of the DNA bundle in *Paramyrothecium roridum* using the primers ITS1 and ITS4 was 562 base pairs. In another study by Hassan et al, 2020, it was established that the PCR amplification results were of the size of 557–603 base pairs of DNA samples extracted from *Paramyrothecium roredium.*

Sequencing and Sequence Alignment

After the PCR reaction was completed amplifying the target of interest, the DNA bundle was sliced from the agarose gel, placed in an Eppendorf tube, and treated with the forward primer and deionized water using a specific extraction kit. The Korean Microgen Company received this sample to determine its nucleotide sequence by the Sanger method. Direct submission of nucleotide sequences to the Gene Bank. (Fig: 19).

Nitrogenous base sequencing results

The PCR reaction's amplified bundles from the fungal isolate were transmitted to the Korean Microgen company so that the sequence and order of nitrogenous bases could be compared to the original gene at certain sites by the Sanger hypothesis According to Table(1), there are 20 and 34 locations where the nucleotide sequence of sample 1 and 2 differ from the original gene on the NCBI site; the two samples were not identical, and 92% similarity to other samples in the NCBI database as shown in table (2,3) and (Fig: 19). For the first sample as the results shown in (Fig: 16) genetic variation due to changes in nitrogenous base composition at certain locations 137 and 246 whence it occurred transversion thymine T into adenine A as well as thymine T into guanine G was seen at site 140 and adenine A into cytosine C at sites 170 and 343 also cytosine C into adenine A at sites 172, 193 and 319

and adenine A into thymine T at sites 199 and 320 and cytosine C into guanine G at site 315. Regarding the nitrogenous bases transition the action of the nitrogenous base replacement C with T was seen at sites 138, 150, 164,186 and 324 also thymine T with cytosine C in 148 and guanine G with adenine in 224, 233, and 260. Similarly, a tranversion of the nitrogen bases was seen in the second sample (Fig. 17), in positions 125 and 193, where cytosine C is converted to adenine A, and adenine A into cytosine C in 127 and 170, and adenine A into thymine T in 128, 199, 254, 320, 337, and guanine G into cytosine C in 298, and cytosine C into guanine G in 315, 379, 421, 494, and thymine T into guanine G in 405, 406, and thymine T into adenine A in 469 and 508. concerning transition, it showed up in 150, 164, 186, 203, 319, 324, 393, 407, and 417 wherein cytosine C was substituted by the nitrogen base thiamine T, also in locations 198, 224, 260, 428 wherein guanine G was replaced with adenine A and the nitrogen base thiamine T was substituted by cytosine C in location 328, 381, 454.

Table (1): Locations of genetic variation in the ITS gene sequences of *Paramyrothecium roridum* isolate.

Myrothecium roridum						
Sample	Type of substitution	Location	Nucleotide	Sequence ID with compare	Source	Identities
1	Gap	119	`A	ID: JF724152.1	*Myrothecium roridum* strain MA-20 18S ribosomal RNA gene	92%
	Gap	124	C			
	Gap	125	C			
	Gap	132	C			
	Gap	134	T			
	Transversion3	137	A/T			
	Transition	138	T/C			
	Transversion	140	G/T			
	Transition	148	C/T			
	Transition	150	T/C			
	Transition	164	T/C			
	Transversion	170	C/A			
	Transversion	172	a/C			
	Transition	186	t/c			
	Transversion	193	a/c			
	Transversion	199	T/A			
	Gap	208	T			
	Transition	224	A/G			
	Gap	225	A			
	Transition	233	A/G			
	Transversion	246	A/T			
	Transition	260	A/G			
	Transversion	315	G/C			
	Transversion	319	A/C			
	Transversion	320	T/A			
	Transition	324	T/C			
	Transversion	343	C/A			
	Gap	346	T			

Sample	Type of substitution	Location	Nucleotide	Sequence ID with compare	Source	Identities
2	Gap	119	A	ID: JF724152.1	Myrothecium roridum strain MA-20 18S ribosomal RNA gene	92%
	Transversion	125	A/C			
	Transversion	127	C/A			
	Transversion	128	T/A			
	Transition	150	T/C			
	Transition	164	T/C			
	Gap	167	A			
	Transversion	170	C/A			
	Transition	186	T/C			
	Transversion	193	A/C			
	Transition	198	A/G			
	Transversion	199	T/A			
	Transition	203	T/C			
	Gap	205	G			
	Transition	224	A/G			
	Gap	225	A			
	Transversion	254	T/A			
	Transition	260	A/G			
	Transversion	298	C/G			
	Transversion	315	G/C			
	Transition	319	T/C			
	Transversion	320	T/A			
	Transition	324	T/C			
	Transition	328	C/T			
	Transversion	337	T/A			
	Gap	345	T			
	Transversion	379	G/C			
	Transition	381	C/T			
	Gap	388	C			
	Gap	391	C			
	Transition	393	T/C			
	Gap	395	T			
	Transversion	405	G/T			
	Transversion	406	G/T			
	Transition	407	T/C			
	Transition	417	T/C			
	Transversion	421	G/C			
	Transition	428	A/G			
	Transition	454	C/T			
	Transversion	469	A/T			
	Transversion	494	G/C			
	Gap	495	G			
	Transversion	508	A/T			

Table (2): The percentage of agreements among the copies that were specifically identified and the other copies in NCBI for sample 1.

Score	Expect	Identities	Gaps	Strand
466 bits(252)	7e-136	312/340(92%)	8/340 (2%)	Plus/Minus

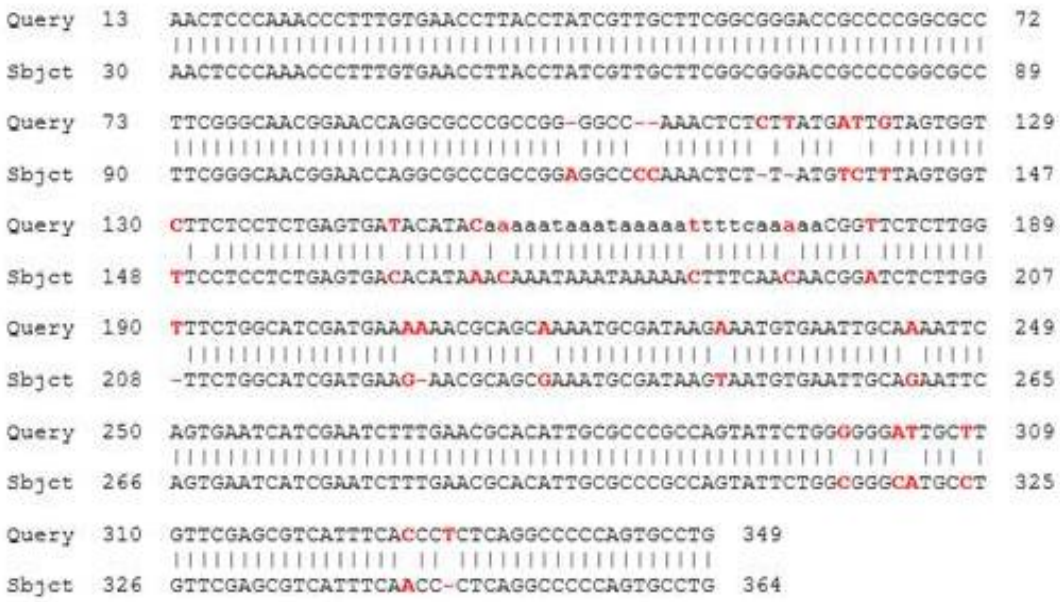

Fig (16): Explanation of the sites of genetic variation in the nucleotide chains of the first sample of *Paramyrothecium roridum*

Table (3): The percentage of agreement among the copies that were specifically identified and the other copies in NCBI for sample 2.

Score	Expect	Identities	Gaps	Strand
726 bits(393)	0.0	484/527(92%)	9/527 (1%)	Plus/Minus

```
Query  1    AACCCTTTGTGAACCTTACCTATCGTTGCTTCGGCGGGACCGCCCCGGCGCCTTCGGGCA  60
            ||||||||||||||||||||||||||||||||||||||||||||||||||||||||||||
Sbjct  38   AACCCTTTGTGAACCTTACCTATCGTTGCTTCGGCGGGACCGCCCCGGCGCCTTCGGGCA  97

Query  61   ACGGAACCAGGCGCCCGCCGG-GGCCCAACTCTCTTATGTCTTTAGTGGTTTTCTCCTCT  119
            |||||||||||||||||||||  |||||  |  ||||||||||||||||||||  |||||||
Sbjct  98   ACGGAACCAGGCGCCCGCCGGAGGCCCCAAACTCTTATGTCTTTAGTGGTTTCCTCCTCT  157

Query  120  GAGTGATAC-TACACAAATAAATAAAAATTTTCAAAAACGATTCTTTTGGGTTCTGGCAT  178
            ||||||  ||  ||  ||||||||||||||  ||||||  ||||   |||  ||  ||||||||||||
Sbjct  158  GAGTGACACATAAACAAATAAATAAAAACTTTCAACAACGGATCTCTT-GGTTCTGGCAT  216

Query  179  CGATGAAAAAACGCAGCGAAATGCGATAAGTAATGTGATTTGCAAAATTCAGTGAATCAT  238
            |||||||  ||||||||||||||||||||||||||||||  |||||  ||||||||||||||||
Sbjct  217  CGATGAAG-AACGCAGCGAAATGCGATAAGTAATGTGAATTGCAGAATTCAGTGAATCAT  275

Query  239  CGAATCTTTGAACGCACATTGCCCCCGCCAGTATTCTGGGGGGTTTGCTTGTCCGAGCGT  298
            ||||||||||||||||||||||  ||||||||||||||||  |||  |||  |||  |||||||
Sbjct  276  CGAATCTTTGAACGCACATTGCGCCCGCCAGTATTCTGGCGGGCATGCCTGTTCGAGCGT  335

Query  299  CTTTTCAACCTCTCAGGCCCCCAGTGCCTGGCGTTGGGGATCGGGGCGGGCTC-GG-GTA  356
            |  ||||||||  ||||||||||||||||||||||||||||||||  |  ||||||  ||  |  |
Sbjct  336  CATTTCAACC-CTCAGGCCCCCAGTGCCTGGCGTTGGGGATCGGCGTGGGCTCCGGCGCA  394

Query  357  TCCCTCCGGGGGGGTGCCGCGTGCTTGCGGGCCCCAAAATTCAGTGGCGGTCTCGCTGTAG  416
              ||||||||||   |||||||||  |||  ||||||  ||||||||||||||||||||||||
Sbjct  395  -CCCTCCGGGGGTTCGCCGCGTGCCTGCCGGCCCCGAAATTCAGTGGCGGTCTCGCTGTAG  453

Query  417  CCCCCCTCTGCGTAGAAGCACAACTCGCATTGGAGCTCGGGGGGTGGCCATGCCGAAAAA  476
            ||||||||||||||  ||||||||||||||||||||||||  ||||||||||||  ||||
Sbjct  454  TCCCCCTCTGCGTAGTAGCACAACTCGCATTGGAGCTCGGC-GGTGGCCATGCCGTAAAA  512

Query  477  CACCCCACTTCTGAAAGTTGACCTCGGATCAGGTAGGAATACCCGCT  523
            |||||||||||||||||||||||||||||||||||||||||||||||
Sbjct  513  CACCCCACTTCTGAAAGTTGACCTCGGATCAGGTAGGAATACCCGCT  559
```

Fig (17): Explanation of the sites of genetic variation in nucleotide chains of the second sample of *Paramyrothecium roridum*

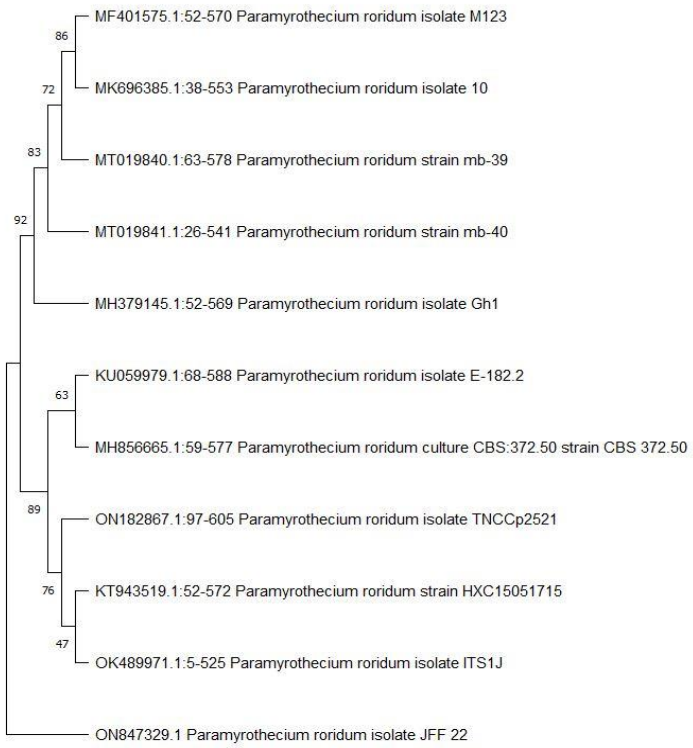

Figure (18): the genetic dimension and affinity tree for the *JFF22 Paramyrothecium roridum* has been registered with the NCBI

Figure (19): The registration process of the new fungus species Paramyrothecium *roridum JFF22*, which has been assigned the identification number ON847329.1

Impact of the media type on the development of *Paramyrothecium roridum JFF22*.

The media outlets contributed to the development of the fungus to varying degrees. Mycelial growth peaked on day 14 on PDA and was lowest on ZA (Figure 20). The rate of expansion was calculated according to colony size per day across all media variations. (Table 4). The most rapid growth rate was observed on PDA, which was notably higher than the rates observed on other media like MEA and Czapek-Dox Agar.

Impact of temperature on the development of *Paramyrothecium roridum JFF22*.

To determine the optimal growth temperature, experiments were conducted using the highest growth potential media PDA on day 7 of incubation. The effect of temperature on radial growth was found to be particularly significant. The largest colony growth of 2 cm was observed at 25 °C (Figure 21). At 20, 30, and 10 °C, colony growth was 1.5, 1.8, and 1 cm, respectively. The smallest colony growth (1 cm) was recorded at 10 °C.

Table (4): Mean of growth rate (Cm/day) of *P. roredium JFF22 in different media*

Media kind	Average diameter of fungal colonies) cm/day)
PDA	4.9
SA	4.5
MEA	4.3
ZA	2.6

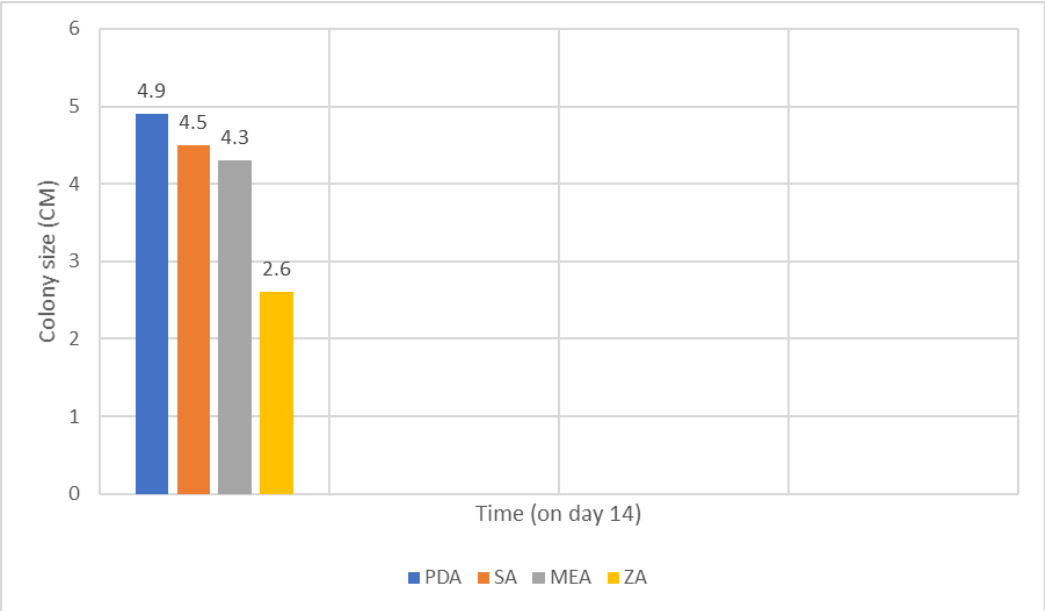

Fig (20): Growth profile of *P. roridum JFF22* in four different media kinds.

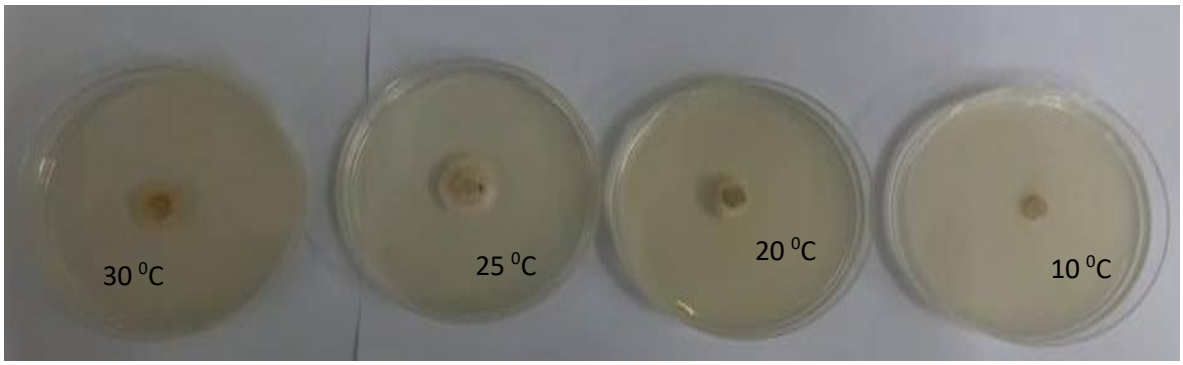

Fig (21): the effect of four temperatures (10, 20, 25, 30) ºC on the growth of *Paramyrothecium roridum JFF22*.

ACKNOWLEDGEMENTS

The authors express their deep gratitude to Northern Technical University, College of Agricultural Technology, Plant Production Techniques, Mosul University, Science College, and Biology Department, the facilities they provided significantly enhanced the quality of this work.

Conflict of interest: None

Funding: None

References

1. Chen, Y.; Ran, S.F.; Dai, D.Q.; Wang, Y.; Hyde, K.D.; Wu, Y.M. and Jiang, Y.L. (2016). Mycosphere Essays 2. *Myrothecium*. Mycosphere 7(1), 64–80. **Doi 10.5943/mycosphere/7/1/7.**
2. Waill, A. E. and Ghoson, M. D. (2019).*Myrothecium* as Promising Model for Biotechnological Applications, Potentials and Challenges. Biomed J Sci & Tech Res 16(3): 12126- 12131.**DOI: 10.26717/BJSTR.2019.16.002869**.
3. Soliman, M. S. (2020). Characterization of *Paramyrothecium roridum* (Basionym *Myrothecium roridum*) causing leaf spot of strawberry. Journal of Plant Protection Research 60 (2):141 – 149. **DOI: 10.24425/jppr.2020.133308**.
4. Matić S, Gilardi G, Gullino ML, Garibaldi A. Emergence of Leaf Spot Disease on Leafy Vegetable and Ornamental Crops Caused by *Paramyrothecium* and *Albifimbria* Species. Phytopathology. 2019 Jun;109(6):1053-1061. **doi: 10.1094/PHYTO-10-18-0396-R. Epub 2019 Apr 24. PMID: 30667339.**
5. Alam, M. W., Rehman, A., Saira, M., Aslam, S., Hameed, A., Sarfraz, S., Muhammad, S., and Riaz, K. 2017. First report of leaf spot caused by *Myrothecium roridum* on watermelon in Pakistan. **Plant Dis.** 101:1053. https://doi.org/10.1094/PDIS-12-16-1812-PDN Link, ISI, Google Scholar
6. Ben, H.-Y., Qu, H.-Y., and Gao, W. 2015a. First report of *Myrothecium roridum* causing brown spot disease on Hiemalis begonia in China. **Plant Dis.** 99:1866. https://doi.org/10.1094/PDIS-03-15-0337-PDN Link, ISI, Google Scholar
7. Ben, H.-Y., Zhao, Y.-J., Chai, A.-L., Shi, Y.-X., Xie, X.-W., and Li, B.-J. 2015b. First report of *Myrothecium roridum* causing leaf spot on *Anthurium andraeanum* in China. **J. Phytopathol.** 163:144-147. https://doi.org/10.1111/jph.12264 Crossref , ISI, Google Scholar
8. Ben, H.-Y., Qu, H.-Y., Chen, L.-X., Zhang, J.-M., Ma, J., Zhang, X.-Y., Zhao, Y.-J., and

Huang, D.-Y. 2017. First report of *Myrothecium roridum* causing leaf spot on *Petunia hybrida* in China. Plant Dis. 101:1956. https://doi.org/10.1094/PDIS-11-16-1570-PDN Link, ISI, Google Scholar

9. Farr, D. F., and Rossman, A. Y. 2018. Fungal Databases, U.S. National Fungus Collections, U.S. Department of Agriculture Agricultural Research Service. https://nt.ars-grin.gov/fungaldatabases/ Google Scholar

10. Fujinawa, M. F., Pontes, N. C., do Vale, H. M. M., Santos, N. F., and Halfeld-Vieira, B. A. 2016. First report of *Myrothecium roridum* causing Myrothecium leaf spot on Begonia in Brazil. Plant Dis. 100:655. https://doi.org/10.1094/PDIS-09-15-1097-PDN Link, ISI, Google Scholar

11. Haudenshield, J. S., Pawlowski, M., Miranda, C., and Hartman, G. L. 2018. First report of *Paramyrothecium roridum* causing Myrothecium leaf spot on soybean in Ghana. **Plant** Dis. 102:2638. https://doi.org/10.1094/PDIS-04-18-0624-PDN Link, ISI, Google Scholar

12. Jordan, B., Culbreath, A. K., Brock, J., and Dutta, B. 2018. First report of Myrothecium leaf spot caused by *Myrothecium roridum* on pepper in the United States. **Plant Dis.** 102:246. https://doi.org/10.1094/PDIS-06-17-0918-PDN Link, ISI, Google Scholar

13. Li, B.-J., Chai, A.-L., and Ben, H.-Y. 2015. First report of *Myrothecium roridum* causing leaf spot of Swedish ivy in China. Plant Dis. 99:1447. https://doi.org/10.1094/PDIS-03-15-0323-PDN Link, ISI, Google Scholar

14. Ye W, Chen Y, Li H, Zhang W, Liu H, et al. (2016) Two trichothecene mycotoxins from *Myrothecium roridum* induce apoptosis of HepG-2 cells via caspase activation and disruption of mitochondrial membrane potential. Molecules 21(6):78.

15. Waill A Elkhateeb, Ghoson M Daba. *Myrothecium* as Promising Model for Biotechnological Applications, Potentials and Challenges. Biomed J Sci & Tech Res 16(3)-2019. BJSTR. MS.ID.002869.

16. Chen Y, Ran SF, Dai DQ, Wang Y, Hyde KD, Wu YM, Jiang YL 2016 – Mycosphere Essays 2. Myrothecium. Mycosphere 7(1), 64–80, Doi 10.5943/mycosphere/7/1/7.

17. Han KS, Choi SK, Kim HH, Lee SC, Park JH, et al. (2014) First report of *Myrothecium roridum* causing leaf and stem rot disease on *Peperomia quadrangularis* in Korea. Mycobiology 42(2): 203-205.

18. Rameshkumara, G.; Sikhab, M.; Ponlakshmia,M.; pandiyana, A.S. and Lalithaa,P.(2019). A rare case of Myrothecium species causing mycotic keratitis: Diagnosis and management. Medical Mycology Case Reports 25 (2019) 53–55.

19. Patidar P (2016) Studies on the *Myrothecium* leaf blight of Cotton incited by *Myrothecium roridum* Tode ex. Fries (Doctoral dissertation, RVSKVV, Gwalior (MP).

20. Norman DJ, Ali S (2013) Ornamental dicus diseases: identification and control in commercial greenhouse operations. University of Florida 308: 1-7.

21. Domsh KH GW, Anderson TH (2007) Compendium of soil fungi. IHW-Verlag, Eching, Germany, pp. 672.

22. Matić S, Gilardi G, Gullino ML, Garibaldi A. Emergence of Leaf Spot Disease on Leafy Vegetable and Ornamental Crops Caused by *Paramyrothecium* and *Albifimbria* Species. Phytopathology. 2019 Jun;109(6):1053-1061. doi: 10.1094/PHYTO-10-18-0396-R. Epub 2019 Apr 24. PMID: 30667339.

23. Bilal Y, Asad UR, Muhammad S, Saeed A, Arshad H, et al. (2018) Risk of *Myrothecium Roridum* Leaf Spot in Local Cucurbitaceous Crops of Pakistan. JOJ Hortic Arboric 2(1): 555577.

24. Tawfik M. Muhsin, Kauther T. Khalaf & Abdul-Hafiz A. Al-Duboon (2012) Antimicrobial

Bioactive Compound Isolated from the Fungus Myrothecium verrucaria, Journal of Biologically Active Products from Nature, 2:3,151-157, DOI: 10.1080/22311866.2012.10719122

25. Lu CC, Yang JS, Huang AC, Hsia TC, Chou ST, Kuo CL, Lu HF, Lee TH, Wood WG, Chung JG. 2010 – Chrysophanol induces necrosis through the production of ROS and alteration of ATP levels in J5 human liver cancer cells. Molecular Nutrition & Food Research 54 (7), 967–976.

26. Zhu ZY, Yao Q, Liu Y, Si CL, Chen J, Liu N, Lian HY, Ding LN, Zhang YM. 2012 – Highly efficient synthesis and antitumor activity of monosaccharide saponins mimicking components of Chinese folk medicine Cordyceps sinensis. Journal of Asian Natural Products Research 14 (5), 429–435.

27. Liu WZ, Tan H, Pan QL, Li HH, Yan HJ, Tan YZ, Zhang WM. 2014 – Chemical constituents of the mycelia of an endophytic Myrothecium roridum from Pogostemon cablin (Blanco) Benth (in Chinese). Journal of Guangdong Pharmaceutical University 30 (4), 427–429.

28. Wagenaar MM, Clardy J. 2001 – Two new roridins isolated from Myrothecium sp. Journal of Antibiotics 54, 517.

29. Basnet B, Liu L, Chen B, Suleimen Y, Yu H, et al. (2019) Four New Cytotoxic Arborinane-Type Triterpenes from the Endolichenic Fungus *Myrothecium inundatum*. Planta medica.

30. Irzoqy, M. E., Sultan, S. J., Abdallah, O. D., Sultan, S. M., Abdullah, Y. J., & Saadi, A. M. (2024). Inhibitory Effect of Saccharomyces cerevisiae Against Propionibacterium acnes. *Journal of Bioscience and Applied Research*, *10*(3), 385-391.

31. Sultan, S. M., Saady, A. M., & Irzoqy, M. E. (2018). A Comparative Study of the Effect of Alcoholic Extract of Turmeric Plant in Inhibiting the Growth of Candida Albicans. *International Journal of Engineering and Technology*, *7*(4.37), 12-16.

32. Pitt, J.I. and Hocking, A.D. (2009). Fungi and Food spoilage, 3rd ed. Springer., 519 pp.

33. N. Kostadinova, E. Krumova, S. Tosi, Pashova & M. Angelova (2009). Isolation and Identification of Filamentous Fungi from Island Livingston, Antarctica, Biotechnology & Biotechnological Equipment, 23:sup1, 267-270, DOI: 10.1080/13102818.2009.10818416.

34. Tulloc,M.(1972). THE GENUS *MYROTHECIUM* TODE ex FR. *Mycological Papers* .18(130): 1-44.

35. Barnett, H. L. and Hunter, B. B. (2006). Illustrated genera of imperfect fungi. 4th ed. Minnesota, USA: American Phytopathological Society Press.

36. Riddell, R. W. 1950. Permanent stained mycological preparation obtained by slide culture. Mycologia 42:265-270.

37. White T.J., Bruns T., Lee S., Taylor J. 1990. Amplification and direct sequencing of fungal ribosomal RNA genes for phylogenetics. p. 315–322. In: "PCR Protocols: A Guide to Methods and Applications" (M.A. Innis, D.H. Gelfand, J.J. Sninsky, T.J. White, eds.). Academic Press, San Diego,
California, USA.

38. Mohammed, I., Nafea, M., Jawad, R., Abd, D., Aljoubory, H. Evaluation of the effect of green synthesis of Zinc oxide nanoparticles on Candida albicans. *Journal of Bioscience and Applied Research*, 2024; 10(3): 518-529. doi: 10.21608/jbaar.2024.380628

39. Tamura K, Peterson D, Peterson N, Stecher G, Nei M and Kumar S (2011) MEGA5: Molecular evolutionary genetics analysis using maximum likelihood, evolutionary distance, and maximum parsimony methods. Mol. Biol. Evol. 28(10), 2731-2739.